



Contents lists available at ScienceDirect

Journal of Hazardous Materials

journal homepage: www.elsevier.com/locate/jhazmat

Pyrolysed waste materials show potential for remediation of trichloroethylene-contaminated water

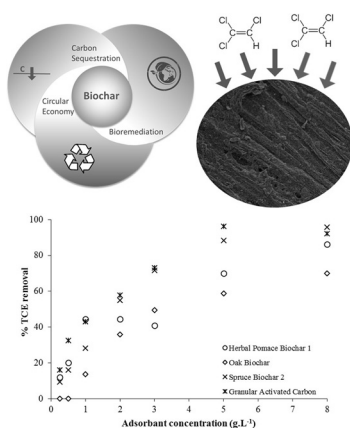
Alma Siggins^{a,b,c,*}, Florence Abram^{a,c}, Mark G. Healy^{b,c}

^a Functional Environmental Microbiology, School of Natural Sciences, National University of Ireland, Galway, Ireland

^b Geo-Environmental Engineering Research, Civil Engineering, National University of Ireland, Galway, Ireland

^c The Ryan Institute, National University of Ireland, Galway, Ireland

GRAPHICAL ABSTRACT



ARTICLE INFO

Editor: Deyi Hous

Keywords:

Trichloroethylene

Biochar

Adsorption

Kinetic study

Circular economy

ABSTRACT

Trichloroethylene (TCE) is an Environmental Protection Agency priority pollutant associated with cancer in humans. With numerous industrial applications and regular landfill disposal, TCE is a common landfill leachate pollutant. *In situ* treatment barriers use costly fill materials such as granular activated carbon (GAC). Here, we show that while a range of untreated waste materials had little ability to adsorb TCE, waste-derived biochar showed excellent capacity for TCE adsorption. TCE removal efficiencies by spruce and oak-derived biochars were > 99.5 %, outperforming GAC (95 %) and herbal pomace biochar (93 %). A contact time of at least 32 h was required to reach equilibrium for all of these media. Assessment of pollution swapping potential revealed release of phosphate by all biochars. Analysis of media surface characteristics by Fourier Transform Infrared Spectroscopy (FTIR) predicted that GAC should have the highest ability to adsorb TCE, followed by Oak Biochar, Herbal Pomace Biochar 1, and Spruce Biochar 2, which was not in agreement with the experimental adsorption data. These data demonstrate the potential for pyrolysed waste material to be used as an alternative fill material for *in situ* remediation applications, thereby also addressing the European Circular Economy Strategy.

* Corresponding author at: Geo-Environmental Engineering Research, Civil Engineering, National University of Ireland, Galway, Ireland.

E-mail address: alma.siggins@nuigalway.ie (A. Siggins).

<https://doi.org/10.1016/j.jhazmat.2019.121909>

Received 17 January 2019; Received in revised form 11 November 2019; Accepted 15 December 2019

0304-3894/ © 2019 Elsevier B.V. All rights reserved.

1. Introduction

Trichloroethylene (TCE; C_2HCl_3 ; CAS Number 79-01-6) is a chlorinated aliphatic compound. It is one of the most frequently identified contaminants in landfill leachate, having been detected in 70 % of 106 landfills tested (Kjeldsen and Christophersen, 2001), and is the contaminant that is typically present in the highest concentration in landfill leachate plumes ($0.05\text{--}750\ \mu\text{g.l}^{-1}$ (Kjeldsen et al., 2002)). Considered to be a priority pollutant, TCE is listed in Annex II, Part B of the European Union Groundwater Directive (European Union, 2006) as being a “man-made synthetic substance”, for which Member States should consider establishing threshold values. By 2017, twenty EU Member States had established such occupational exposure limits for TCE, but the range of limits varies from 0.6 to 100 ppm (EC, 2017).

As TCE has a density of $1.46\ \text{g.ml}^{-1}$, and is therefore heavier than water, environmental contamination tends to move downwards through soil and gravel. This results in the formation of a dense, non-aqueous phase liquid (DNAPL) plume, which may persist for decades and continually desorb from soil and leach into a groundwater source (Wilkin et al., 2014; Bredehoeft, 1992). Options for treating environmental TCE contamination are limited. As DNAPL plumes spread both horizontally and vertically depending on gravity and the direction of water movement through soil, they can cover a large area. Detecting the direction and extent of DNAPL migration is difficult, and current modelling options are limited (Rathfelder et al., 2000). Consequently, physical processes such as removal of soil and venting, or extraction and treatment of pore water are logistically difficult, prohibitively expensive and environmentally disruptive (Bankston et al., 2002). They may also exacerbate the issue, by physically forcing contaminants into less permeable zones, or previously uncontaminated areas (Stroo et al., 2003). Furthermore, contaminants may adsorb to clay particles and be retained in soil following groundwater extraction, only to desorb and persist once the groundwater is recharged. Therefore, focus is increasingly turning to *in-situ* options for remediation, of which adsorption is considered as the best wastewater treatment method due to its universal nature, low cost (depending on the adsorbent employed) and ease of operation (Ali et al., 2012). For decades, activated carbon has been used as an adsorbent for a range of organic compounds including TCE (Ali et al., 2012), as it has a high surface area and a well-defined pore structure (Mattson and Harry, 1971). However, production of activated carbon solely for its use as an adsorbent is potentially unnecessary, and costly, with reports of granular activated carbon (GAC) costing US\$800 – 2500 ton^{-1} (Huggins et al., 2016). Use of waste products from other sources that are capable of adsorbing TCE would contribute to waste minimisation, as well as a lower cost and environmentally sustainable treatment technology. For example, biochar, at a much lower cost than GAC of US\$51 – 381 ton^{-1} (Huggins et al., 2016), has been reported to demonstrate strong potential for TCE adsorption, including biochar produced from waste materials such as buffalo weed, pine needles and peanut shells (Ahmad et al., 2014, 2013a; Ahmad et al., 2012). Those studies reported removals of TCE from aqueous solutions of up to 88 % (Ahmad et al., 2014). It has been suggested that this is due to the high surface area and pore volume that result from the pyrolysis process (Trinh et al., 2017; Mukherjee et al., 2011). However, some studies have reported that biochar may release nutrients, such as nitrogen (N) and phosphorus (P) (Chintala et al., 2014; Qian et al., 2015), which should be carefully considered to minimise environmental impacts such as eutrophication from excess nutrients. In addition to biochar, other raw waste materials have been reported to be capable of adsorption of a range of contaminants, including organic contaminants. Gypsum is a key component of plasterboard, a waste product in the construction industry, and has been shown to be capable of adsorption of the volatile organic contaminants toluene and formaldehyde (Thevenet et al., 2018). Bottom ash and fly ash are by-products of the incineration process, and have been reported to adsorb polychlorinated biphenyls (Nollet et al., 2003) and a range of

azo dyes including Amaranth (Mittal et al., 2005), Acid Orange 7 (Gupta et al., 2006) and Reactive Red 141 (Leechart et al., 2009). Granular blast slag is a by-product of the steel manufacturing industry, capable of adsorption of Malachite Green (Gupta et al., 1997). Peat fibre is highly porous with a large surface area and a high cation capacity, which has been shown to adsorb dyes (Ho and Mckaf, 2000) and metals (Ho et al., 2002). Alum sludge and ferric chloride residue are by-products of the water treatment process capable of adsorbing phosphate (Hou et al., 2018). Bauxite residue is a by-product of the extraction of alumina, which can adsorb arsenic (Soner Altundogan et al., 2000).

The aim of this study was to investigate the potential of a range of high production volume waste media, including biochars derived from waste, for the low-cost *in-situ* adsorption of TCE. Adsorption, kinetics, pollution swapping, and impact of temperature and pH were considered in order to comprehensively assess the media types included in the study.

2. Materials and methods

2.1. Media description

Fifteen media types were assessed for their ability to adsorb TCE. All media were raw (used untreated in the form generated by their respective industries) or pyrolysed waste by-products originating from a range of industry settings and were selected based on criteria such as low cost, bulk availability and potential for local sourcing. Raw materials analysed in this study included gypsum, bottom ash, fly ash, granular blast slag, peat fibre, steel wool, alum sludge, bauxite residue and ferric chloride residue. Two biochars were produced from waste spruce timber feedstock. Spruce Biochar 1 was produced in Ireland, in a rotating kiln at a pyrolysis temperature of 700 °C, with O_2 levels below 4 %, and a residence time of 14 min. Spruce Biochar 2 was produced in Germany using a PYREG plant (www.pyreg.de), at 600 °C and a residence time of approximately 30 min. Two biochars (Herbal Pomace Biochar 1 and 2) were produced from herbal pomace waste, which is the residual material following extraction of essential oils from plants. Although the herbal pomace biochars were sourced from different organisations within Germany, they were both produced using the PYREG system, operated at 600 °C and a residence time of approximately 30 min. The fifth biochar (Oak Biochar) was produced from an oak sawmill waste feedstock, in a cone kiln similar to a Kon-Tiki kiln (Schmidt and Taylor, 2014), and was pyrolysed at 650–720 °C. This system progressively adds the feedstock in layers to the kiln, so retention times may be up to 8 h. As GAC has been shown to strongly adsorb TCE in previous studies, it was included as a benchmark for the waste media (Analab, Ireland; DARCO, 12–20 mesh). All media were dried at 105 °C for 24 h, then crushed or cut to 1–2 mm, prior to starting the experiments.

2.2. Batch experimental design

Equilibration solutions were prepared using TCE ($\geq 99\%$; Analab, Ireland) and sodium azide ($\geq 99.5\%$; Sigma-Aldrich) in distilled water, with stirring for 1 h. Sodium azide was used at a final concentration of 0.02 % w/v to prevent biological degradation of TCE (Pavlostathis and Jaglal, 1991). Batch tests were set up in 40 ml amber glass vials, filled to overflowing with no headspace to prevent TCE volatilisation, and sealed with a PTFE-lined cap. Batch tests were equilibrated for 48 h (unless otherwise stated) on a mechanical reciprocal shaker at 160 rpm at room temperature (approximately $22\ ^\circ\text{C} \pm 2\ ^\circ\text{C}$). The vial-point technique was used, where each vial represented one data point (Salih et al., 2011). Control vials containing no media were included to calculate precise TCE adsorption by each media and account for loss of TCE by other routes, which were minimal.

2.3. Adsorption experimental design

To assess the potential for TCE adsorption over a set time, each of the 15 media was used in 48 h batch tests at an adsorbent dose of 5 g.l⁻¹. Solutions were prepared at TCE concentrations of 2, 20 or 200 mg.l⁻¹ (Analab Ireland; Honeywell, > 99 %) in distilled water.

2.4. Pollution swapping

Pollution swapping is the increase of one pollutant as a result of a measure to decrease a different pollutant. To investigate the potential for release of N and P from the media, 5 g.l⁻¹ media was added to 40 ml distilled water, equilibrated for 48 h and immediately passed through 0.45 µm PTFE-hydrophilic syringe filters. The filtrate was analysed for dissolved reactive phosphorus (DRP) and total oxidised nitrogen (TON) using a nutrient analyser (KoneLab20, Thermo Clinical Labsystems, Finland).

2.5. Media characterisation

The four media types that exhibited the best potential for TCE adsorption after 48 h underwent proximate, ultimate and physical characterisation. Proximate analysis of the media was carried out as described by Ahmed et al. (Ahmad et al., 2014). Ultimate analysis of organic carbon (C_{org}), oxygen (O) and hydrogen (H) was carried out by the manufacturers of the biochar as part of their quality control process as per the German standard methods for solid mineral fuels analysis : DIN 51732 (C, H; (DIN 51732, 2007; DIN 51732, 2007)) and DIN 51733 (O; (DIN 51733, 2008; DIN 51733, 2008)). Molar ratios of H:C_{org} and O:C_{org} were calculated from these data. Physical and morphological analyses were carried out by Glantreo LTD (Cork, Ireland). SEM analysis was carried out to ASTM 766 and E1508 standards, using an FEI Inspect F, working at 5 kV and a working distance of approximately 9 mm.

Fourier Transform Infrared Spectroscopy (FTIR) spectra analysis was carried out to identify functional groups on the surface of the biochars, using a PerkinElmer Spectrum 400 (Waltham, Massachusetts) equipped with a DATR 1 bounce Diamond/ZnSe Universal ATR sampling accessory. Spectra were measured in the range from 4000 to 650 cm⁻¹ with eight accumulations and 4 cm⁻¹ resolution.

2.6. Impact of pH on TCE adsorption

The impact of pH on the adsorption capabilities of the four biochars were assessed at a TCE concentration of 200 mg.l⁻¹ and an adsorbent dose of 5 g.l⁻¹. The TCE solution was prepared as described in Section 2.2, and then aliquoted into three portions as follows: i) unadjusted (approximately pH 7), ii) buffered to pH 5 with HCl, and iii) buffered to pH 9 with NaOH.

2.7. Adsorption capability

The adsorption capability of the four selected biochars were assessed across an adsorbent mass range of 0.25–12.5 g.l⁻¹, using a synthetic TCE solution with sodium azide (as per Section 2.2) at a TCE concentration of 200 mg.l⁻¹. The data were modelled by linear and non-linear Langmuir (Langmuir (1916)), Freundlich (Freundlich (1906)), Koble-Corrigan (Koble and Corrigan, 1952), Temkin (Vijayaraghavan et al., 2006) and Dubinin-Radushkevich (Vijayaraghavan et al., 2006) adsorption isotherms using Excel's Solver plugin to determine the best fitting parameters by minimising the residual sum of squares for the non-linear models. The Hanes-Woolf form was used for the linearised Langmuir model (Supplementary Table 1; (Hanes, 1932)). The goodness of fit of all models was assessed by calculating the coefficient of determination (r^2 ; Eq. 1) and the non-linear models were also assessed by calculation of the chi-squared value (χ^2 ;

Eq. 2). High r^2 and low χ^2 values are indicative that the data are a good fit to the model.

$$r^2 = 1 - \frac{\sum (q_{exp} - q_{calc})^2}{\sum (q_{exp} - q_{exp.mean})^2} \quad (1)$$

$$\chi^2 = \sum \frac{(q_{exp} - q_{calc})^2}{q_{calc}} \quad (2)$$

Where: q_{exp} is the experimental sorption capacity (mg.g⁻¹), q_{calc} is the modelled sorption capacity (mg.g⁻¹), and $q_{exp.mean}$ is the mean of the experimental sorption capacities.

2.8. Kinetic study

The selected biochars were assessed for the rate at which they adsorb TCE from the solution using a kinetic study. A synthetic TCE solution with sodium azide was prepared as described in Section 2.2, at a TCE concentration of 200 mg.l⁻¹, and all kinetic batch vials were established at an adsorbent concentration of 5 g.l⁻¹. Replicate vials for each biochar were destructively sampled at 10 time points: 0, 1, 3, 4, 8, 12, 18, 24, 32 and 48 h. The values for time point zero were determined by adding a TCE solution to the biochar in vials, and to a no-biochar control vial, followed by immediate filtration and analysis. The contact time was only several seconds and is reported as 0 h. The data were fitted to the linear version of first and second order (Ahmad et al., 2013b), pseudo first (Lagergren, 1898) and pseudo second order (Ho and McKay, 1999), Elovich (Roginsky and Zeldovich, 1934) and intraparticle diffusion (McKay and Poots, 1980) kinetic equations (Supplementary Table 3). The coefficient of determination (r^2 ; Eq. 1) and standard error of estimates (SEE; Eq. 3) values were used to investigate the goodness of fit for the kinetic models. A high r^2 and low SEE are indicative that the data are a good fit to the model.

$$SEE = \sqrt{\frac{(\sum q_{exp} - \sum q_{calc})^2}{(n - 2)}} \quad (3)$$

Where: q_{exp} is the experimental sorption capacity (mg.g⁻¹), q_{calc} is the modelled sorption capacity (mg.g⁻¹), and $q_{exp.mean}$ is the mean of the experimental sorption capacities.

2.9. Analytical methods

Following equilibration, the solutions from each batch test vial from the 48 h experiment (Section 2.3), the pH experiment (section 2.6), the adsorption experiment (section 2.7) and the kinetic experiment (section 2.8), were immediately filtered through 0.45 µm PTFE-hydrophilic syringe filters to separate the adsorbent from the liquid samples. Duplicate 100 µl aliquots of the filtrates were added to 10 ml distilled water in 20 ml headspace vials, crimp sealed, and analysed by static headspace using a CombiPAL headspace autosampler, followed by gas chromatography (CP-3800, Varian, Palo Alto, CA) with a mass spectrometer detector using the following method: Headspace equilibration at 80 °C, 500 rpm, 5 min; then one ml headspace transferred to the injector by heated syringe (90 °C); injector temperature 240 °C, initial oven temperature 50 °C (1 min) ramping to 200 °C at 40 °C min⁻¹, and holding for 1 min (total cycle time 5.75 min). Helium was used as the carrier gas at 1 ml.min⁻¹. Separation was carried out on a DB 624 Ultra Inert Capillary column, 20 m length x0.18 mm internal diameter x1 µm film thickness (Agilent Technologies, Germany). Standard stocks of TCE in methanol were prepared at 100X concentration at least monthly. Calibration curves of known TCE concentrations were constructed and used to determine concentrations of TCE in the samples, expressed as mg.l⁻¹.

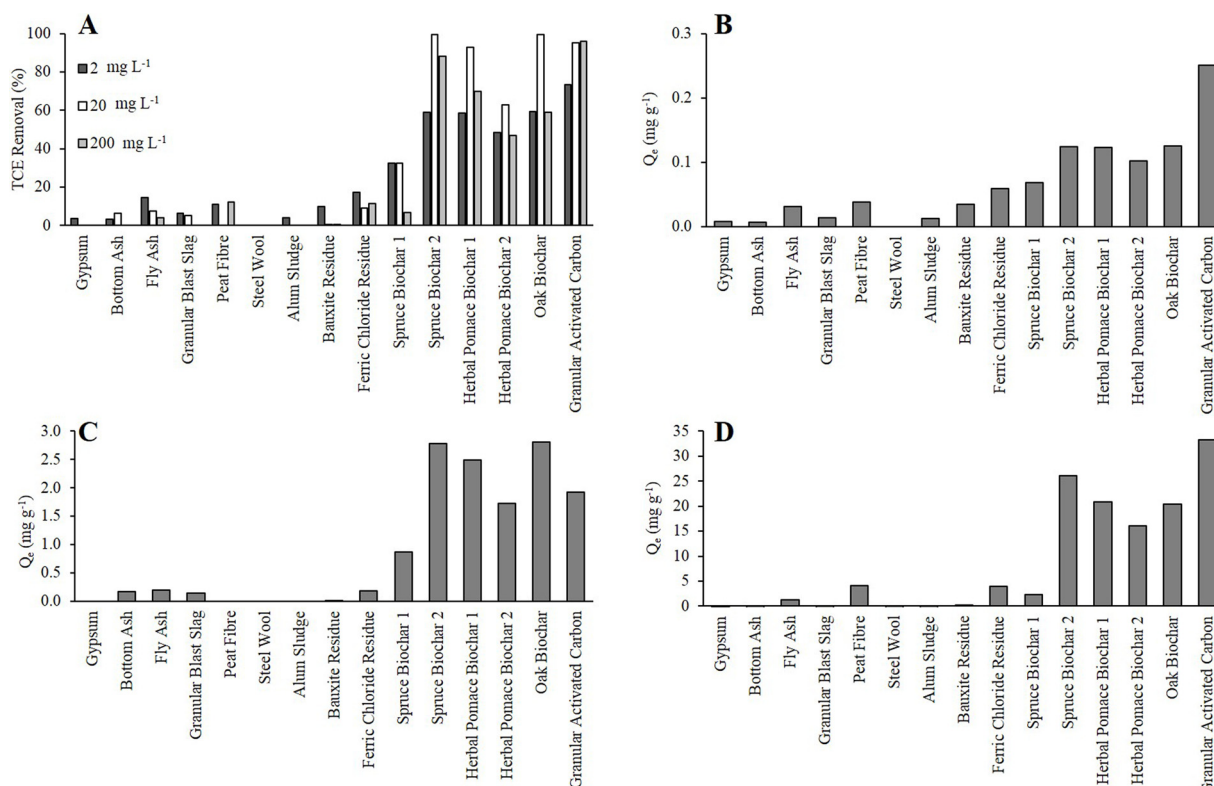


Fig. 1. TCE removal by 15 raw or pyrolysed waste media at an adsorbent concentration of 5 g.L^{-1} , following equilibration for 48 h at room temperature ($22 \text{ }^\circ\text{C} \pm 2 \text{ }^\circ\text{C}$), shaking at 160 rpm. A: % TCE removal at initial TCE concentrations of 2, 20 and 200 mg.L^{-1} , where % removal was determined by comparison to a no-media vial containing the same TCE solution and subjected to the same experimental conditions (shaking time/speed) as the test vials; B-D: Amount of TCE (mg) adsorbed per gram of each media from an initial TCE concentration of 2 mg.L^{-1} (B) 20 mg.L^{-1} (C) or 200 mg.L^{-1} (D).

3. Results and discussion

3.1. Batch tests: total adsorption over 48 h

The raw (*i.e.* unpyrolysed) media showed limited potential for adsorption of TCE from aqueous solutions (Fig. 1). Ferric chloride residue and fly ash were the only raw media to adsorb TCE across all three initial concentrations investigated (Fig. 1). Of these, ferric chloride residue performed best, removing 17, 8 and 11 % of TCE from the 2, 20 and 200 mg.L^{-1} solutions, respectively (Fig. 1).

Biochar and GAC performed better than the raw media (Fig. 1), removing up to 99.5 % of TCE from the aqueous solution. The two biochars produced from a Sitka spruce feedstock demonstrated very different TCE adsorption capacities, as Spruce Biochar 1 only had a maximum TCE removal capacity of 30 %, while Spruce Biochar 2 adsorbed over 99.5 % TCE (Fig. 1), which was equivalent to the minimum detection limit of TCE remaining in solution. For all biochar and GAC, the TCE concentration in the initial solution is directly proportional to adsorption capacity (Fig. 1b–d), which is likely to be a result of the increased chemical driving force of the concentration gradient (Ata et al., 2012).

3.2. Pollution swapping

The fifteen media were analysed for potential to leach nutrients that could result in negative environmental impacts such as eutrophication of surface or groundwater. Alum sludge was the only media to release N in the form of TON, at a concentration of 300 mg kg^{-1} (data not shown). None of the biochars in our study demonstrated any leaching of TON under the experimental conditions investigated. Extremely low release of N ($< 1 \text{ mg.kg}^{-1}$) from biochar has previously been reported (Gaskin et al., 2008; Mukherjee and Zimmerman, 2013), and the

formation of insoluble ‘black N’ during the pyrolysis process has also been attributed to low potential for N leaching from biochar (Knicker, 2010).

Many of the raw media and GAC demonstrated little ($< 10 \text{ mg.kg}^{-1}$) or no release of DRP (Fig. 2). However, phosphate release in the range of $29\text{--}1854 \text{ mg.kg}^{-1}$ was observed from the biochars (Fig. 2). These are in agreement with the range of $46\text{--}1664 \text{ mg.kg}^{-1}$ previously reported by biochars derived from similar feedstocks including oak, pine and grass (Mukherjee and Zimmerman, 2013). Phosphate concentrations $> 0.02 \text{ mg.l}^{-1}$ are considered to potentially lead to increased algal growth and eutrophication (US EPA, 1995). All five biochars resulted in leached phosphate concentrations between

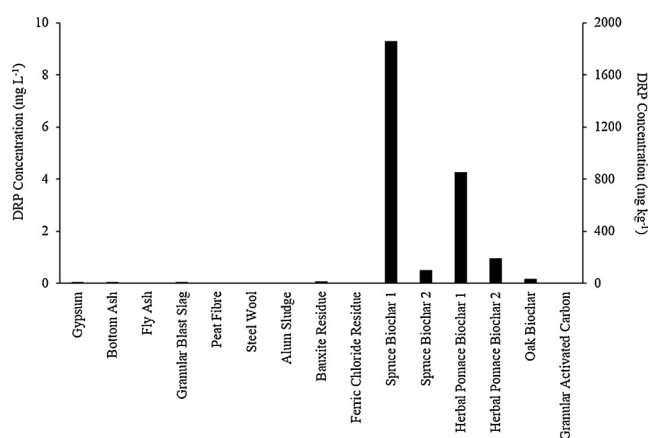
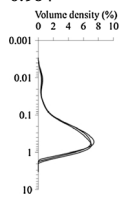
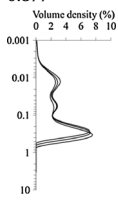
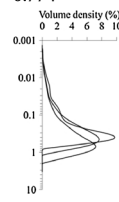
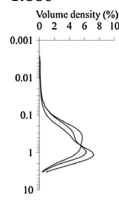


Fig. 2. Phosphate release by the media, expressed as Dissolved Reactive Phosphorus (DRP) concentration at equilibrium (mg.L^{-1} , primary vertical axis) and DRP leached per kg media (mg.kg^{-1} , secondary vertical axis).

Table 1
Characterisation of best performing media.

	Herbal Pomace Biochar 1	Oak Biochar	Spruce Biochar 2	Granular Activated Carbon
Proximate analysis				
Moisture content (%)	22.3	9.3	27.0	4.7
Mobile matter (%)	16.7	11.8	16.1	5.1
Resident matter (%)	51.7	74.5	44.6	79.2
Ash (%)	9.3	4.4	12.3	11.0
Ultimate Analysis ^a				
O (%)	6.9	5.4	2.8	19.9
C _{org} (%)	66.6	82.7	74.3	78.1
H (%)	0.91	0.98	0.97	1.51
Molar H/C _{org}	0.16	0.14	0.16	0.23
Molar O/C _{org}	0.006	0.004	0.002	0.016
Physical and Morphological Analysis ^b				
BET Surface Area (m ² g ⁻¹)	374	216	39	633
Pore Diameter (nm)	6	12	39	9
Pore Volume (cm ³ g ⁻¹)	0.03	0.001	0.001	0.48
Particle Size Distribution (mm)				
D ₁₀	0.085	0.009	0.047	0.133
D ₅₀	0.387	0.113	0.332	0.583
D ₉₀	0.964	0.377	0.774	1.660
Size classes (mm)				
				

^a biochar data provided by respective biochar manufacturer; Granular activated carbon obtained from literature values [66].

^b Analysis carried out by Glantreo Ltd.

0.16 and 9.28 mg.l⁻¹, at an adsorbent dose of 5 g.l⁻¹ (Fig. 2). Therefore, the incorporation of these media into an environmental bioremediation strategy should carefully consider the quantity of biochar required, the potential groundwater movement through the site, and the location of water systems that may be vulnerable to eutrophication.

3.3. Media characterisation

The characteristics of the best performing media are shown in Table 1. Typically, studies investigating the suitability of biochar for use as an adsorbent focus on the production of biochar from a single feedstock under varied pyrolysis conditions. In those cases, the pyrolysis temperature has a strong impact on the adsorption capability of the biochars, with increased pyrolysis temperature associated with lower yield, mobile matter and oxygen content, and higher ash content, resident matter, organic carbon, Brunauer-Emmett-Teller (BET) surface area and pore volume (Ahmad et al., 2013a, 2012; Mohan et al., 2014). The biochars in the current study were all produced at high temperatures (> 600 °C) and therefore should have good potential for TCE adsorption. Indeed, the pyrolysis conditions were reasonably consistent across all biochars, so it is unlikely that the production parameters will have a significant impact on the TCE adsorption capacity of the biochars. Conversely, the biochars were all produced from different feedstocks, which is more likely to impact the adsorption properties of the final product. The three biochars were all produced from plant-based feedstock, but these were green material (herbal pomace), hardwood (oak) and softwood (spruce). The feedstock appears to affect the proximate data for the biochars, with the Oak Biochar having a lower moisture and ash content and higher resident matter than the Herbal Pomace Biochar 1 or Spruce Biochar 2 (Table 1). Overall, the mobile matter content of all media analysed was low (5–17 %; Table 1), with up to 46 % mobile matter reported for other plant-based biochars (Ahmad et al., 2014). Mobile matter content is associated with microbial activity, and the low levels present in these biochars indicate that they should be resistant to microbial degradation. Conversely, the high resident matter content of the biochars indicates that they are stable

and much of the organic matter is fully carbonised (Ahmad et al., 2012). With regards to the ultimate analysis data, all media had a high C_{org} and would be classified as “Class I” by the International Biochar Initiative (IBI), which requires > 60 % C_{org} (International Biochar Initiative, 2015). The molar H:C_{org} ratio gives an indication of the degree of carbonisation, aromaticity and stability of biochar. All of the biochars investigated were below the threshold (0.7) to show complete thermochemical conversion. Molar O:C_{org} is also used as a quality control parameter related to the presence of polar functional groups and surface hydrophobicity, and associated with biochar stability, with values of < 0.4 required by the IBI (International Biochar Initiative, 2015). Biochar with O:C_{org} > 0.6 is considered to be susceptible to microbial degradation, with a half-life in soil of < 100 years, while biochar with O:C_{org} < 0.2 has a predicted half-life of > 1000 years (Spokas, 2010). The biochars investigated all had an O:C_{org} < 0.02, which is in agreement with the low mobile matter content finding that they would be resistant to microbial degradation. A low O:C_{org} is an important characteristic if the biochar is to be used for long-term, *in situ* bioremediation strategies.

Biochars typically have a heterogenous surface, with a combination of micro-, meso- and macropores. All of the media had average pore diameters in the mesopore range (2–50 nm; Table 1). Smaller pores are considered to be desirable for adsorption to increase contact points, but a minimum pore diameter 1.7 times that of the adsorbate is required to prevent size exclusion (Li et al., 2019). The kinetic diameter of TCE is 0.56 nm (Li et al., 2019), so this would equate to a theoretical minimum pore diameter of approximately 1 nm. All of the media had average pore diameters > 1 nm (Table 1), which should be sufficient for TCE adsorption.

With the exception of the spruce-derived biochar, all media had a high surface area (Table 1). A BET surface area > 150 m². g⁻¹ is associated with good adsorption potential (EBC, 2016). The four media had different particle size distributions, with Oak Biochar having the lowest mean values (D₅₀), followed by Spruce Biochar 2, then Herbal Pomace Biochar 1, and finally the highest D₅₀ values were associated with GAC (Table 1). Particle size has been shown to have a greater

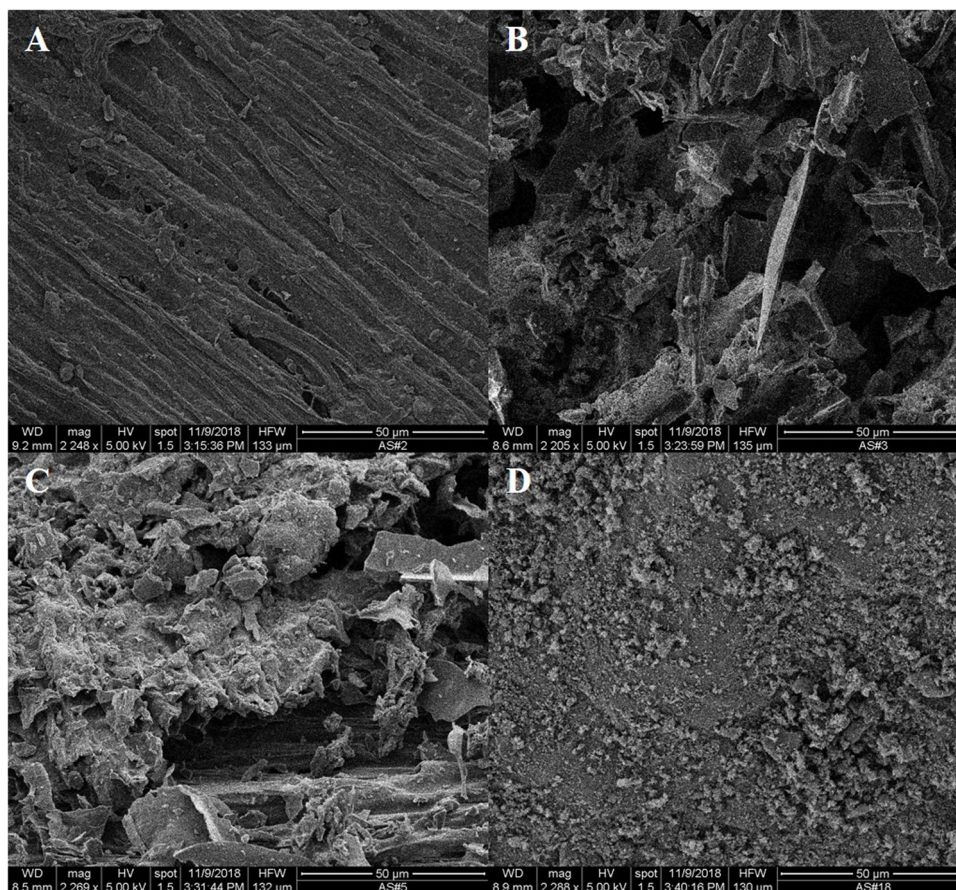


Fig. 3. Scanning electron micrographs with 50 µm scale bars of A Herbal Pomace Biochar 1; B Oak Biochar; C Spruce Biochar 2; D Granular activated carbon.

influence on the adsorption capacity of biochar than BET surface area, with smaller particles being more effective adsorbents (Han et al., 2016). This is associated with the presence of pores, leading to an overall heterogeneous surface area, which alters the relationship between particle size and surface area. For example, Crini et al. reported particle sizes in the range of 150–250 µm as having a BET surface area of 2.4 m²·g⁻¹, while particles twice that size (300–500 µm) had a BET surface area of 1.5 m²·g⁻¹ (Crini et al., 2007). SEM imaging (Fig. 3) confirmed highly variable, small-scale structures of the media surfaces indicating that although particle size would typically be inversely related to surface area, the proportion of this relationship would vary by media type.

Since all samples were char-based, FTIR background interference and baseline offset were higher than usual. Because of this, a Standard Normal Variate pre-treatment was applied to the spectra using the software package “R” to allow spectra to be compared, and subsequently differences between samples were observed (Fig. 4). Assignments of functional groups to peaks were carried out based on Coates (Coates (2000)). GAC showed little, if any, information having high baseline offset with a few minor shoulders at 1537 cm⁻¹ and 1228 cm⁻¹. This is expected, as charcoal is known to absorb almost all information within the IR region with very little emittance. The media with most deviation was Spruce Biochar 2, having a broad peak at 3350 cm⁻¹, most likely from O–H or N–H stretching, though the additional amine peak at 1583 cm⁻¹ would suggest N–H stretching from a primary amine. A peak at 1394 cm⁻¹ is more than likely due to an N–O bond, but may also be from C–O. Peaks at around 1010 cm⁻¹ are more than likely from C–O and/or C–N. The sharp peak at 870 cm⁻¹ is more than likely from aromatic C–H stretching. Herbal Pomace Biochar 1 spectra were similar to Spruce Biochar 2, though the peaks are less intense and the broad peak at 3350 cm⁻¹ is absent. This indicates a

similar compound on the surface of the Herbal Pomace Biochar 1 samples. Oak Biochar showed less peak intensity with shoulders at 1583 cm⁻¹ and 1394 cm⁻¹, and the sharp 870 cm⁻¹ peak detected in Spruce Biochar 2 and Herbal Pomace Biochar 1 is greatly reduced and is barely observable. The most observable peak in the Oak Biochar spectra was the broad hump at ≈ 1010 cm⁻¹. The pyrolysis process has been reported to result in the removal of O and H-containing functional groups, increasing the surface hydrophobicity of biochar (Ahmad et al., 2014; Chun et al., 2004), which should promote the adsorption of hydrophobic molecules such as TCE (Karanfil and Dastgheib, 2004). From the FTIR spectra obtained from the media, it would be expected that GAC should have the highest ability to adsorb TCE, followed by Oak Biochar, Herbal Pomace Biochar 1, then Spruce Biochar 2.

3.4. Batch tests: impact of pH

The pH of the aqueous solution is one of the most significant parameters that influences the adsorption process, as it affects the surface charge and speciation of the target compound (Tan et al., 2015). However, Erto et al. reported little to no impact of pH on TCE adsorption onto the surface of activated carbon (Erto et al., 2010). As such, pH was only briefly considered in this study, to assess if all media displayed optimal TCE adsorption capacity at any one specific pH value. This was not the case as the four media demonstrated varied responses to changes in pH. Herbal Pomace Biochar 1 and GAC both had a significantly ($p < 0.05$) higher adsorption capacity for TCE at pH 7, while Spruce Biochar 2 was significantly lower at pH 7 (Fig. 5). Oak Biochar demonstrated good adsorption across all pH values investigated (Fig. 5). In general, as no consistently optimal pH was observed across all media, the decision was made not to adjust the pH of the TCE solution for subsequent batch tests, which were carried out without

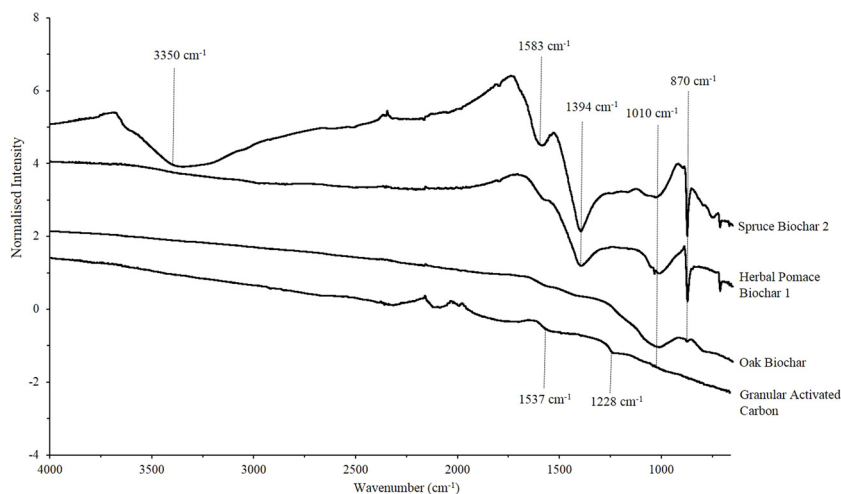


Fig. 4. Fourier Transform Infrared Spectroscopy (FTIR) spectra of Herbal Pomace Biochar 1, Oak Biochar, Spruce Biochar 2 and Granular activated carbon. Fourier Transform Infrared Spectroscopy (FTIR) spectra analysis was carried out using a PerkinElmer Spectrum 400 (Waltham, Massachusetts) equipped with a DATR 1 bounce Diamond/ZnSe Universal ATR sampling accessory. Spectra were measured in the range from 4000 to 650 cm^{-1} with 8 accumulations and 4 cm^{-1} resolution.

buffering at pH 6.8.

3.5. TCE Adsorption over a range of media concentrations

As expected from the characterisation data in section 3.3, GAC removed the most TCE from the aqueous solution, with 96.2 % removal at an adsorbent dose of 5 g.L^{-1} (Fig. 6A). Increasing the adsorbent dose to 8 g.L^{-1} did not improve TCE removal by GAC, which decreased to 92.1 % at this concentration (Fig. 6A). This trend was not observed with the three biochars, which consistently showed that the highest adsorbent dose resulted in the best TCE removal (Fig. 6A). Of the three biochars analysed, Spruce Biochar 2 demonstrated the highest TCE removal at 8 g.L^{-1} (95.7 %), followed by Herbal Pomace Biochar 1 (86.2 %), and finally Oak Biochar (70 %; Fig. 6A). The amount of TCE adsorbed per gram of media (Q_e) was also determined (Fig. 6B). In general, lower media concentrations resulted in higher Q_e values. The highest Q_e value (97.8 mg.g^{-1}) was recorded for GAC at an adsorbent concentration of 0.25 g.L^{-1} , followed by Herbal Pomace Biochar 1 (72.0 mg.g^{-1} at 0.25 g.L^{-1}), then Spruce Biochar 2 (59.0 mg.g^{-1} at 0.25 g.L^{-1}). No TCE removal was observed at 0.25 or 0.5 g.L^{-1} of Oak Biochar, which had the highest Q_e (27.4 mg.g^{-1}) at the 2 g.L^{-1} adsorbent concentration (Fig. 6B). This is somewhat in agreement with the findings of Wei & Seo (Wei and Seo, 2010), who demonstrated that non-pyrolysed pine mulch was a better adsorbent material for TCE than hardwood mulch. However, that study found that this was probably due to higher C_{org} content in pine compared to hardwood, which were reported as 51 % and 43 %, respectively (Wei and Seo, 2010). In the current study, the C_{org} of all biochars would be considered to be “high” (66–82 %; Table 1). Several studies originating from one group investigating TCE adsorption on biochars produced under different conditions have reported maximum

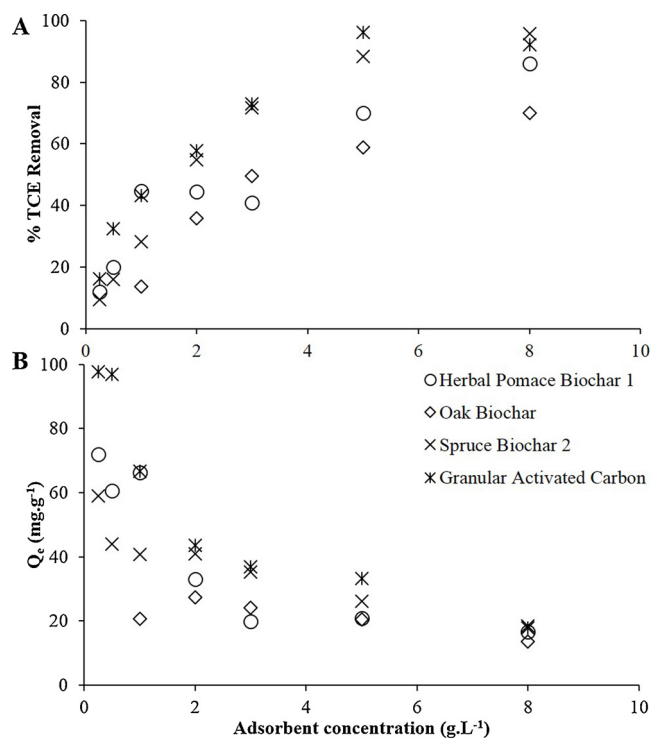


Fig. 6. TCE removal over a range of media concentrations, expressed as (A) % TCE removal and (B) amount of TCE adsorbed per gram of media (Q_e). The adsorption study was carried out at a TCE concentration of 200 mg.L^{-1} and an equilibrium time of 48 h.

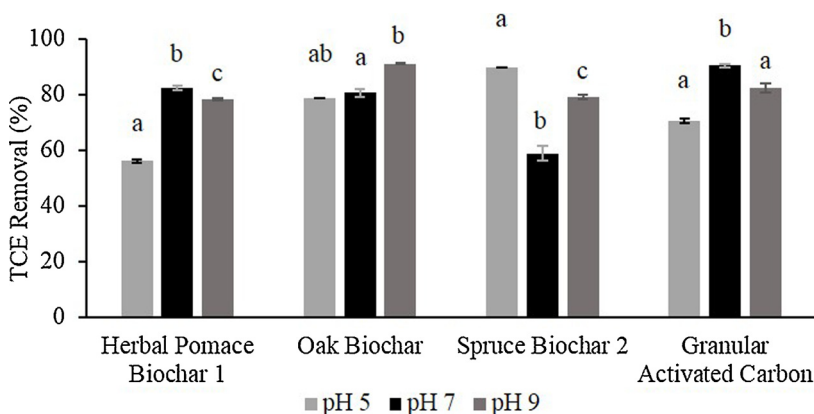


Fig. 5. Impact of aqueous solution pH on TCE adsorption by selected media. Error bars represent standard error (stdev/\sqrt{n} , where n is the number of replicates). Lower case letters indicate statistically significant difference ($p < 0.05$) in Q_e as a result of pH within each media, calculated by one-way Anova using Excel’s data analysis plug-in. The impact of pH on the adsorption capabilities of the four media were assessed at a TCE concentration of 200 mg.L^{-1} , an adsorbent dose of 5 g.L^{-1} , and an equilibrium time of 48 h.

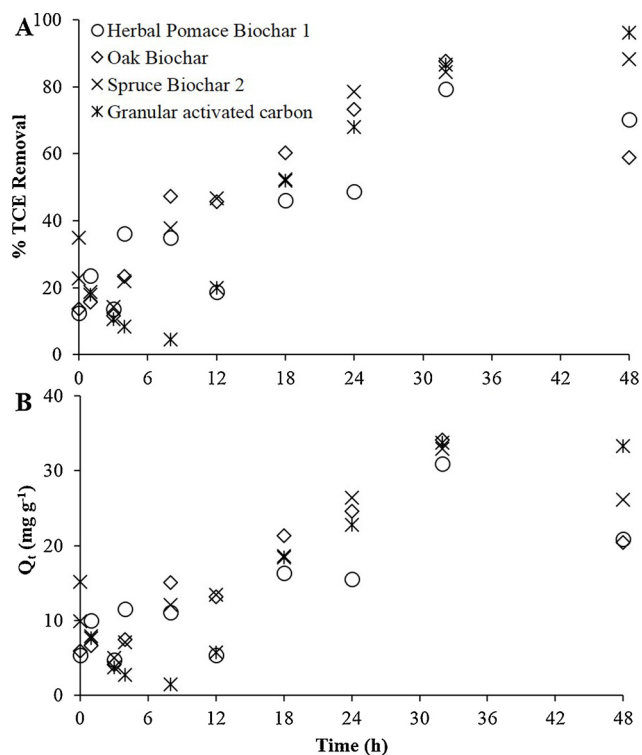


Fig. 7. TCE adsorption kinetics on selected biochars. Q_t is the amount of TCE adsorbed by the media at a given time point. The kinetic study was carried out at a TCE concentration of 200 mg L^{-1} , and an adsorbent concentration of 5 g L^{-1} . Replicate vials for each media were destructively sampled at 10 time points: 0, 1, 3, 4, 8, 12, 18, 24, 32 and 48 h.

Q_e values for a range of feedstocks such as pine needles (Q_e ca. 100 mg g^{-1} ; (Ahmad et al., 2013c)), buffalo weed (Q_e ca. 90 mg g^{-1} ; (Ahmad et al., 2014)), peanut shell (Q_e 30 mg g^{-1} ; (Ahmad et al., 2012)) and soybean stover (Q_e 25 mg g^{-1} ; (Ahmad et al., 2012)). Those studies reported C content of 94, 82, 84 and 85 %, respectively, but these are reported as total carbon, and not as the organic fraction. Assessment of C_{org} , as opposed to total C, is recommended by the IBI due to the potential presence of inorganic carbonates in high-ash biochars (International Biochar Initiative, 2015). The poor performance of Oak Biochar was not predicted by FTIR data, which showed relatively low levels of surface functional groups for this medium (Fig. 4). However, the FTIR spectra did predict that Herbal Pomace Biochar 1 would have a higher capacity for TCE adsorption than Spruce Biochar 2 (Fig. 4). Although the data were fitted to multiple adsorption isotherms (Supplementary Tables 1 & 2), the quality of the fit of the experimental data to the modelled isotherm was highly variable. As such, no meaningful conclusions could be drawn from the modelling approach. Although the number of studies investigating adsorption of TCE by biochar is limited, the current study is generally in agreement with the literature (Ahmad et al., 2012; Erto et al., 2010; Ahmad et al., 2013c).

3.6. Batch test: kinetic study

Maximum TCE adsorption appears to have been reached for all media by 32 h of contact time (Fig. 7A & B). By 32 h, the TCE removal from the aqueous solution ranged from 79 to 88 % for all four media (Fig. 7A). Comparison of the quantity of TCE adsorbed by the media at a given time point (Q_t), shows that in general this value decreased between 32 h and 48 h (Fig. 7B). However, it is possible that this is a feature of individual batch test vials being analysed per sample point, rather than extracting an aliquot from a single vessel at each time point. This approach is required for TCE adsorption studies, to prevent loss of

TCE by volatilisation into a headspace that would increase in volume over the course of the experiment if aliquots were removed (Ahmad et al., 2012, 2013c). After 32 h, the four media demonstrated similar Q_t values ($31\text{--}34 \text{ mg g}^{-1}$), although Herbal Pomace Biochar 1 typically had a lower Q_t than the other media at other time points, and Oak Biochar demonstrated better adsorption at earlier time points (Fig. 7A & B). Interestingly, none of the media demonstrated the two-phase adsorption characterised by a fast initial adsorption stage followed by a slower stage, which has been previously reported in kinetic adsorption studies (Ahmad et al., 2013b). As with the adsorption data, the experimental kinetic data were fitted to a range of kinetic models, but the goodness of fit of the data was variable and limited the value of the parameters derived from the models (Supplementary Tables 3 & 4).

4. Conclusions

The raw waste materials investigated demonstrated little capability for TCE adsorption from aqueous solutions, with less than 20 % TCE removal observed. Conversely, the three best performing biochars shortlisted for further analysis displayed strong adsorbent characteristics, including a low particle size, $H:C_{\text{org}}$ and $O:C_{\text{org}}$; high surface area, pore volume and pore diameter. At a starting concentration of 20 mg l^{-1} , two of the waste-derived biochars were capable of adsorbing > 99.5 % TCE, which was greater than the 95 % TCE removal by GAC. Kinetic studies showed that the majority of adsorption had occurred after 32 h. Overall, the data indicate that the biochars investigated would be suitable for remediation of a TCE-contaminated aqueous solution, but the raw waste materials examined in our study would not be appropriate for this purpose.

Declaration of Competing Interest

None.

Acknowledgements

This project has received funding from the European Union's Horizon 2020 research and innovation programme under the Marie Skłodowska-Curie Actions grant agreement No 748106. The authors would like to acknowledge laboratory assistance from Tatiana Kelley, NUI Galway and RPS, FTIR analysis by Pól Mac Fhionnghaile, School of Chemistry, NUI Galway, and biochar contributions from: Prof JJ Leahy, University of Limerick, Ireland; Caspar von Ziegner, NovoCarbo, Germany; Timo Ferdinand, HerbaCarbo, Germany, and Thomas Fleming, Brooko GbR, Germany.

Appendix A. Supplementary data

Supplementary material related to this article can be found, in the online version, at doi:<https://doi.org/10.1016/j.jhazmat.2019.121909>.

References

- Ahmad, M., Lee, S.S., Dou, X., Mohan, D., Sung, J.K., Yang, J.E., Ok, Y.S., 2012. Effects of pyrolysis temperature on soybean stover- and peanut shell-derived biochar properties and TCE adsorption in water. *Bioresour. Technol.* 118, 536–544. <https://doi.org/10.1016/j.biortech.2012.05.042>.
- Ahmad, M., Lee, S.S., Rajapaksha, A.U., Vithanage, M., Zhang, M., Cho, J.S., Lee, S.E., Ok, Y.S., 2013a. Trichloroethylene adsorption by pine needle biochars produced at various pyrolysis temperatures. *Bioresour. Technol.* 143, 615–622. <https://doi.org/10.1016/j.biortech.2013.06.033>.
- Ahmad, M., Lee, S.S., Oh, S.E., Mohan, D., Moon, D.H., Lee, Y.H., Ok, Y.S., 2013b. Modeling adsorption kinetics of trichloroethylene onto biochars derived from soybean stover and peanut shell wastes. *Environ. Sci. Pollut. Res.* 20, 8364–8373. <https://doi.org/10.1007/s11356-013-1676-z>.
- Ahmad, M., Lee, S.S., Rajapaksha, A.U., Vithanage, M., Zhang, M., Cho, J.S., Lee, S.E., Ok, Y.S., 2013c. Trichloroethylene adsorption by pine needle biochars produced at various pyrolysis temperatures. *Bioresour. Technol.* 143, 615–622. <https://doi.org/10.1016/j.biortech.2013.06.033>.

- Ahmad, M., Moon, D.H., Vithanage, M., Koutsospyros, A., Lee, S.S., Yang, J.E., Lee, S.E., Jeon, C., Ok, Y.S., 2014. Production and use of biochar from buffalo-weed (*ambrosia trifida* L.) for trichloroethylene removal from water. *J. Chem. Technol. Biotechnol.* 89, 150–157. <https://doi.org/10.1002/jctb.4157>.
- Ali, I., Asim, M., Khan, T.A., 2012. Low cost adsorbents for the removal of organic pollutants from wastewater. *J. Environ. Manage.* 113, 170–183. <https://doi.org/10.1016/j.jenvman.2012.08.028>.
- Ata, S., Imran Din, M., Rasool, A., Qasim, I., Ul Mohsin, I., 2012. Equilibrium, thermodynamics, and kinetic sorption studies for the removal of coomassie brilliant blue on wheat bran as a low-cost adsorbent. *J. Anal. Methods Chem.* 1. <https://doi.org/10.1155/2012/405980>.
- Bankston, J.L., Sola, D.L., Komor, A.T., Dwyer, D.F., 2002. Degradation of trichloroethylene in wetland microcosms containing broad-leaved cattail and eastern cottonwood. *Water Res.* 36, 1539–1546. [https://doi.org/10.1016/S0043-1354\(01\)00368-2](https://doi.org/10.1016/S0043-1354(01)00368-2).
- Bredehoeft, J., 1992. Much contaminated groundwater can't be cleaned up. *Ground Water* 30, 834–835. <https://doi.org/10.1111/j.1745-6584.1992.tb01564.x>.
- Chintala, R., Schumacher, T.E., McDonald, L.M., Clay, D.E., Malo, D.D., Papiernik, S.K., a Clay, S., Julson, J.L., 2014. Phosphorus sorption and availability from biochars and soil/biochar mixtures. *Clean - Soil Air Water* 42, 626–634. <https://doi.org/10.1002/clean.201300089>.
- Chun, Y., Sheng, G., Chiou, G.T., Xing, B., 2004. Compositions and sorptive properties of crop residue-derived chars. *Environ. Sci. Technol.* 38, 4649–4655. <https://doi.org/10.1021/es035034w>.
- Coates, J., 2000. Interpretation of infrared spectra, a practical approach. In: Meyers, R. (Ed.), *Encycl. Anal. Chem.* John Wiley & Sons Ltd, Chichester, pp. 10815–10837. <https://doi.org/10.5860/choice.36-5697>.
- Crini, G., Peindly, H.N., Gimbert, F., Robert, C., 2007. Removal of C.I. basic green 4 (Malachite Green) from aqueous solutions by adsorption using cyclodextrin-based adsorbent: kinetic and equilibrium studies. *Sep. Purif. Technol.* 53, 97–110. <https://doi.org/10.1016/j.seppur.2006.06.018>.
- DIN 51732, 2007. Testing of Solid Mineral Fuels - Determination of Total Carbon, Hydrogen and Nitrogen - Instrumental Methods.
- DIN 51733, 2008. Testing of Solid Mineral Fuels - Ultimate Analysis and Calculation of Oxygen Content.
- EBC, 2012. European Biochar Certificate - Guidelines for a Sustainable Production of Biochar 2016. Eur. Biochar Found. (EBC), Arbaz, Switzerland, pp. 1–22. <https://doi.org/10.13140/RG.2.1.4658.7043>. Version 6.1 19th June.
- EC, 2017. Commission Staff Working Document Impact Assessment. Accompanying the Document Proposal for a Directive of the European Parliament and of the Council Amending Directive 2004/37/EC on the Protection of Workers from the Risks Related to Exposure to Carcinogens.
- Erto, A., Andreozzi, R., Di Natale, F., Lancia, A., Musmarra, D., 2010. Experimental and statistical analysis of trichloroethylene adsorption onto activated carbon. *Chem. Eng. J.* 156, 353–359. <https://doi.org/10.1016/j.cej.2009.10.034>.
- European Union, 2006. Ground Water Directive. <https://eur-lex.europa.eu/LexUriServ/LexUriServ.do?uri=OJ:L:2006:372:0019:0031:EN:PDF>.
- Freundlich, H.M.F., 1906. Über Die Adsorption in Lösungen. *Z. Phys. Chem.* 57, 385–470.
- Gaskin, J., Steiner, C., Harris, K., Das, K.C., Bibens, B., 2008. Effect of low-temperature pyrolysis conditions on biochar for agricultural use. *Am. Soc. Agric. Biol. Eng.* 51, 2061–2069. <https://doi.org/10.13031/2013.25409>.
- Gupta, V.K., Srivastava, S.K., Mohan, D., 1997. Equilibrium uptake, sorption dynamics, process optimization, and column operations for the removal and recovery of malachite green from wastewater using activated carbon and activated slag. *Ind. Eng. Chem. Res.* 36, 2207–2218. <https://doi.org/10.1021/ie960442c>.
- Gupta, V.K., Mittal, A., Gajbe, V., Mittal, J., 2006. Removal and recovery of the hazardous azo dye acid orange 7 through adsorption over waste materials: bottom ash and de-oiled soya. *Ind. Eng. Chem. Res.* 45, 1446–1453. <https://doi.org/10.1021/ie051111f>.
- Han, Y., Cao, X., Ouyang, X., Sohi, S.P., Chen, J., 2016. Adsorption kinetics of magnetic biochar derived from peanut hull on removal of Cr(VI) from aqueous solution: effects of production conditions and particle size. *Chemosphere* 145, 336–341. <https://doi.org/10.1016/j.chemosphere.2015.11.050>.
- Hanes, C.S., 1932. Studies on plant amylases: the effect of starch concentration upon the velocity of hydrolysis by the amylase of germinated barley. *Biochem. J.* 26, 1406–1421.
- Ho, K.S., Mckay, G., 2000. The kinetics of sorption of basic dyes from aqueous solution by Sphagnum moss peat. *Can. J. Chem. Eng.* 76.
- Ho, Y.S., McKay, G., 1999. Pseudo-second order model for sorption processes. *Process Biochem.* 34, 451–465. [https://doi.org/10.1016/S0032-9592\(98\)00112-5](https://doi.org/10.1016/S0032-9592(98)00112-5).
- Ho, Y.S., Porter, J.F., McKay, G., 2002. Equilibrium isotherm studies for the sorption of divalent metal ions onto peat: copper, nickel and lead single component systems. *Water Air Soil Pollut.* 141, 1–33. <https://doi.org/10.1023/A:1021304828010>.
- Hou, Q., Meng, P., Pei, H., Hu, W., Chen, Y., 2018. Phosphorus adsorption characteristics of alum sludge: Adsorption capacity and the forms of phosphorus retained in alum sludge. *Mater. Lett.* 229, 31–35. <https://doi.org/10.1016/j.matlet.2018.06.102>.
- Huggins, T.M., Haeger, A., Biffinger, J.C., Ren, Z.J., 2016. Granular biochar compared with activated carbon for wastewater treatment and resource recovery. *Water Res.* 94, 225–232. <https://doi.org/10.1016/j.watres.2016.02.059>.
- International Biochar Initiative, 2015. Standardized Product Definition and Product Testing Guidelines for Biochar That Is Used in Soil. <https://doi.org/10.1016/j.zefq.2013.07.002>.
- Karanfil, T., Dastgheib, S.A., 2004. Trichloroethylene adsorption by fibrous and granular activated carbons: Aqueous phase, gas phase, and water vapor adsorption studies. *Environ. Sci. Technol.* 38, 5834–5841. <https://doi.org/10.1021/es0497936>.
- Kjeldsen, P., Christophersen, M., 2001. Composition of leachate from old landfills in Denmark. *Waste Manage. Res.* 19, 249–256. <https://doi.org/10.1177/0734242X0101900306>.
- Kjeldsen, P., Barlas, M.A., Rooker, A.P., Baun, A., Ledin, A., Christensen, T.H., 2002. Present and long-term composition of MSW landfill leachate: a review. *Crit. Rev. Environ. Sci. Technol.* 32, 297–336. <https://doi.org/10.1080/10643380290813462>.
- Knicker, H., 2010. Organic geochemistry ‘Black nitrogen’ – an important fraction in determining the recalcitrance of charcoal. *Org. Geochem.* 41, 947–950. <https://doi.org/10.1016/j.orggeochem.2010.04.007>.
- Koble, R.A., Corrigan, T.E., 1952. Adsorption isotherms for pure hydrocarbons. *Ind. Eng. Chem.* 44, 383–387.
- Lagergren, S., 1898. About the theory of so-called adsorption of soluble substance. *K. Sven. Vetensk. Handl.* 24, 1–39.
- Langmuir, I., 1916. Constitution and fundamental properties of solids and liquids. I. *Solids. J. Am. Chem. Soc.* 38, 2221–2295.
- Leechart, P., Nakbanpote, W., Thiravetyan, P., 2009. Application of “waste” wood-shaving bottom ash for adsorption of azo reactive dye. *J. Environ. Manage.* 90, 912–920. <https://doi.org/10.1016/j.jenvman.2008.02.005>.
- Li, L., Quinlivan, A., Patricia, R.U., 2019. Knappe, Detlef, effects of activated carbon surface chemistry and pore structure on the adsorption of organic contaminants from aqueous solutions. *Carbon N. Y.* 40 (2AD), 2085–2100.
- Mattson, J.S., Harry, B.M., 1971. Activated Carbon: Surface Chemistry and Adsorption From Solution.
- McKay, G., Poots, V.J., 1980. Kinetics and diffusion processes in colour removal from effluent using wood as an adsorbent. *J. Chem. Technol. Biotechnol.* 30, 279–292.
- Mittal, A., Kurup, L., Gupta, V.K., 2005. Use of waste materials - bottom ash and de-oiled soya, as potential adsorbents for the removal of Amaranth from aqueous solutions. *J. Hazard. Mater.* 117, 171–178. <https://doi.org/10.1016/j.jhazmat.2004.09.016>.
- Mohan, D., Sarswat, A., Ok, Y.S., Pittman, C.U., 2014. Organic and inorganic contaminants removal from water with biochar, a renewable, low cost and sustainable adsorbent - a critical review. *Bioresour. Technol.* 160, 191–202. <https://doi.org/10.1016/j.biortech.2014.01.120>.
- Mukherjee, A., Zimmerman, A.R., Harris, W., 2011. Surface chemistry variations among a series of laboratory-produced biochars. *Geoderma* 163, 247–255. <https://doi.org/10.1016/j.geoderma.2011.04.021>.
- Mukherjee, A., Zimmerman, A.R., 2013. Organic carbon and nutrient release from a range of laboratory-produced biochars and biochar – soil mixtures. *Geoderma* 193–194, 122–130. <https://doi.org/10.1016/j.geoderma.2012.10.002>.
- Nollet, H., Roels, M., Lutgen, P., Van Der Meer, P., Verstraete, W., 2003. Removal of PCBs from wastewater using fly ash. *Chemosphere* 53, 655–665. [https://doi.org/10.1016/S0045-6535\(03\)00517-4](https://doi.org/10.1016/S0045-6535(03)00517-4).
- Pavlostathis, S.G., Jaglal, K., 1991. Desorptive behavior of trichloroethylene in contaminated soil. *Environ. Sci. Technol.* 25, 274–279. <https://doi.org/10.1021/es00014a009>.
- Qian, K., Kumar, A., Zhang, H., Bellmer, D., Huhnke, R., 2015. Recent advances in utilization of biochar. *Renew. Sustain. Energy Rev.* 42, 1055–1064. <https://doi.org/10.1016/j.rser.2014.10.074>.
- Rathfelder, K.M., Lang, J.R., Abriola, L.M., 2000. A numerical model (MISER) for the simulation of coupled physical, chemical and biological processes in soil vapor extraction and bioventing systems. *J. Contam. Hydrol.* 43, 239–270. [https://doi.org/10.1016/S0169-7722\(00\)00086-3](https://doi.org/10.1016/S0169-7722(00)00086-3).
- Roginsky, S., Zeldovich, Y.B., 1934. The catalytic oxidation of carbon monoxide on manganese dioxide. *Acta Phys. Chem. USSR* 1, 554.
- Salih, H.H., Patterson, C.L., Sorial, G.A., Sinha, R., Krishnan, R., 2011. The fate and transport of the SiO₂ nanoparticles in a granular activated carbon bed and their impact on the removal of VOCs. *J. Hazard. Mater.* 193, 95–101. <https://doi.org/10.1016/j.jhazmat.2011.07.030>.
- Schmidt, H.P., Taylor, P., 2014. Kon-Tiki flame curtain pyrolysis for the demercaptization of biochar production. *Biochar J.* q 14–24.
- Soner Altundogan, H., Altundogan, S., Tümen, F., Bildik, M., 2000. Arsenic removal from aqueous solutions by adsorption on red mud. *Waste Manage.* 20, 761–767. [https://doi.org/10.1016/S0956-053X\(00\)00031-3](https://doi.org/10.1016/S0956-053X(00)00031-3).
- Spokas, K.A., 2010. Review of the stability of biochar in soils: predictability of O:C molar ratios. *Carbon Manage.* 1, 289–303. <https://doi.org/10.4155/cmt.10.32>.
- Stroo, H.F., Unger, M., Ward, C.H., Kavanaugh, M.C., Vogel, C., Leeson, A., Marqusee, J.A., Smith, B.P., 2003. Remediating chlorinated solvent source zones. *Environ. Sci. Technol.* 37, 224A–230A.
- Tan, X., Liu, Y., Zeng, G., Wang, X., Hu, X., Gu, Y., Yang, Z., 2015. Application of biochar for the removal of pollutants from aqueous solutions. *Chemosphere* 125, 70–85. <https://doi.org/10.1016/j.chemosphere.2014.12.058>.
- Thevenet, F., Debono, O., Rizk, M., Caron, F., Verrielle, M., Locoge, N., 2018. VOC uptakes on gypsum boards: sorption performances and impact on indoor air quality. *Build. Environ.* 137, 138–146. <https://doi.org/10.1016/j.buildenv.2018.04.011>.
- Trinh, B.S., Werner, D., Reid, B.J., 2017. Application of a full-scale wood gasification biochar as a soil improver to reduce organic pollutant leaching risks. *J. Chem. Technol. Biotechnol.* <https://doi.org/10.1002/jctb.5219>.
- US EPA, 1995. *USEPA Ecological Restoration: A Tool to Manage Stream Quality.* Report EPA 841-F-95-007, Washington, DC, USA.
- Vijayaraghavan, K., Padmesh, T.V.N., Palanivelu, K., Velan, M., 2006. Biosorption of nickel(II) ions onto *Sargassum wightii*: application of two-parameter and three-parameter isotherm models. *J. Hazard. Mater.* 133, 304–308.
- Wei, Z., Seo, Y., 2010. Trichloroethylene (TCE) adsorption using sustainable organic mulch. *J. Hazard. Mater.* 181, 147–153. <https://doi.org/10.1016/j.jhazmat.2010.04.109>.
- Wilkin, R.T., Acree, S.D., Ross, R.R., Puls, R.W., Lee, T.R., Woods, L.L., 2014. Fifteen-year assessment of a permeable reactive barrier for treatment of chromate and trichloroethylene in groundwater. *Sci. Total Environ.* 468–469, 186–194. <https://doi.org/10.1016/j.scitotenv.2013.08.056>.